“Fruiting Liquid” of Mushroom-Forming Fungi, A Novel Source of Bioactive Compounds : Fruiting-Body Inducer and HIF and Axl Inhibitors

JOURNAL OF AGRICULTURAL AND FOOD CHEMISTRY

Editors' Choice
Open Access

pubs.acs.org/JAFC

Article

"Fruiting Liquid" of Mushroom-Forming Fungi, A Novel Source of Bioactive Compounds – Fruiting-Body Inducer and HIF and Axl Inhibitors

Jing Wu, Kazuki Uchida, Aoto Yoshikawa, Masaru Hashimoto, Mitsuru Kondo, Kenichi Nihei, Mizuki Ishii, Jae-Hoon Choi, Yukihiro Miwa, Chiho Shoda, Deokho Lee, Ayaka Nakai, Toshihide Kurihara, Corina N. D'Alessandro-Gabazza, Masaaki Toda, Taro Yasuma, Esteban C. Gabazza, Hirofumi Hirai, and Hirokazu Kawagishi*

Cite This: *J. Agric. Food Chem.* 2023, 71, 13338–13345

Read Online

ACCESS | Metrics & More | Article Recommendations | Supporting Information

ABSTRACT: In general, mushroom-forming fungi secrete liquid on the surface of mycelia just before fruiting-body formation. However, no researchers in mushroom science have paid attention to the liquid until now. We formulated a hypothesis that the liquid plays an important role(s) in the formation of the fruiting body and produces various bioactive compounds and named it the "fruiting liquid (FL)". Four novel compounds (**1**–**4**) were isolated from FL of *Hypholoma lateritium* and *Hericium erinaceus*. The structures of **1**–**4** except for their stereochemistry were determined by interpretation of MS and NMR data. The absolute configurations of compounds **1**–**4** were determined by quantum chemical calculation of the ECD spectrum, by single-crystal X-ray diffraction analyses, or by chemical syntheses. Compounds **1**, **3**, and **4** induced fruiting body formation of *Flammulina velutipes*. Compound **4** inhibited the activity of hypoxia-inducible factor, and compounds **2**–**4** suppressed receptor tyrosine kinase (Axl) expression.

KEYWORDS: *fruiting liquid, fruiting-body formation inducer, Axl and immune checkpoints inhibitor, hypoxia-inducible factor inhibitor, structure determination, mushroom*

INTRODUCTION

The fruiting body of ascomycetes and basidiomycetes is known as "mushroom". Fruiting bodies produce spores, and the spores germinate and form mycelium. The mycelium produces a primordium that grows into a new fruiting body, and the life cycle continues. In general, mushroom-forming fungi secrete liquid on the surface of mycelia just before formation of fruiting bodies (Figure 1 and Figure S1). However, no researchers in mushroom science have paid attention to the liquid until now. We formulated a hypothesis that the liquid plays important role(s) in fruiting-body formation and produces various bioactive compounds that are not found in mycelia, fruiting bodies, and other parts of the fungi, and named it "fruiting liquid (FL)".

We attempted to find fruiting body-inducers and other bioactive compounds from FL of two cultured fungi, *Hypholoma lateritium* (Kuritake in Japanese, Brick cap in English) and *Hericium erinaceus* (Yamabushitake in Japanese, Lion's mane mushroom in English, Hou-tou-gu in Chinese). It was a very hard work for us to collect the FL because of a very small quantity of FL secreted per culture pot. Eventually, with the help of mushroom cultivators, we were able to collect large amounts of FL (Figure 1).

As a result, four novel compounds (**1**–**4**) were isolated from the two kinds of FL (Figure 2). Here, we describe the isolation, structure determination, and fruiting body inducing activity of the compounds. In addition, we report the inhibitory activity of these compounds against the hypoxia-inducible factor (HIF) and Axl expression.

MATERIALS AND METHODS

Instruments and Materials. ^{1}H NMR spectra (one- and two-dimensional) were recorded on a Jeol lambda-500 spectrometer or JNM-ECZ500R spectrometer at 500 MHz, or Jeol EX-400 spectrometer at 400 MHz, and ^{13}C NMR spectra were recorded on the same instrument at 125 or 100 MHz (Jeol, Tokyo, Japan). HRESIMS spectra were recorded on a JMS-T100LC mass spectrometer (Jeol, Tokyo, Japan). An FT/IR-4100 (Jasco, Tokyo, Japan) was used to record the IR spectra, and the specific rotation values were measured by a Jasco DIP-1000 polarimeter (Jasco, Tokyo, Japan). Medium Pressure Liquid Chromatography (MPLC) was performed with a TLC-flash chromatograph AKROS, Smart Flash EPCLC AI-580S (Yamazen, Tokyo, Japan). HPLC separations were performed with a Jasco Gulliver system using reversed-phase HPLC columns (phenylhexyl and ODS-P, InertSustain, Tokyo, Japan; Cosmosil PBr, Nacalai Tesque, Kyoto, Japan). Silica gel plate (Merck F_{254}), ODS gel plate (Merck F_{254}), and silica gel 60 N (Kanto Chemical, Tokyo, Japan) were used for analytical TLC and for

Received: June 4, 2023
Revised: August 3, 2023
Accepted: August 4, 2023
Published: August 31, 2023

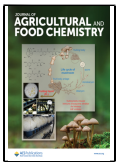

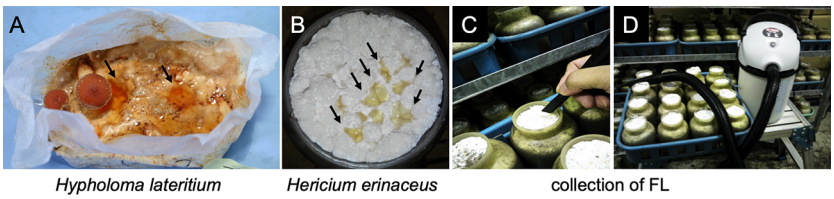

Figure 1. "Fruiting liquid" of *H. lateritium* (A) and *H. erinaceus* (B) and collection of FL using a suction pump (C, D).

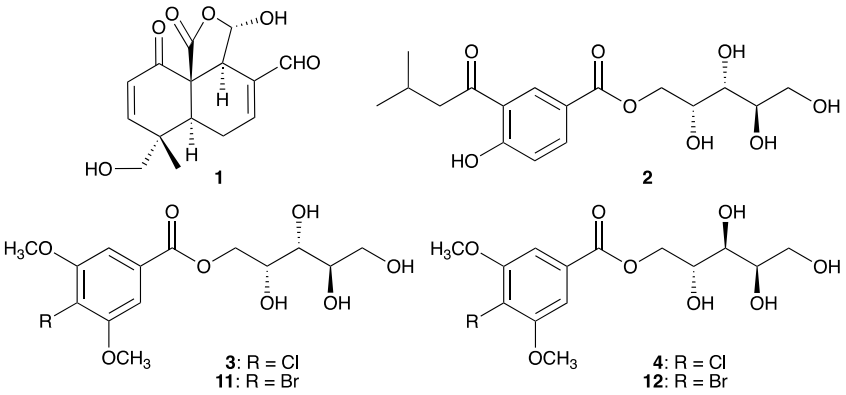

Figure 2. Structures of **1**−**4**, **11**, and **12**.

Table 1. ^{1}H and ^{13}C NMR Data for 1 to 4

	1 (in $CDCl_3$)			**2** (in CD_3OD)			**3** (in CD_3OD)		**4** (in CD_3OD)	
	^{1}H	^{13}C		^{1}H	^{13}C		^{1}H	^{13}C	^{1}H	^{13}C
position	δ_H (mult, *J*, Hz)	δ_C, type	position	δ_H (mult, *J* in Hz)	δ_C, type	position	δ_H (mult, *J* in Hz)	δ_C, type	δ_H (mult, *J* in Hz)	δ_C, type
1		170.9, C	1	-	120.8, C	1	-	130.6, C	-	130.7, C
2	-	-	2	8.59 (d, 2.1)	134.1, CH	2, 6	7.38 (s)	106.7, CH	7.41 (s)	106.8, CH
3	5.35 (d, 12.4)	101.3, CH	3	-	122.3, C	3, 5	-	157.5, C	-	157.5, C
3a	3.62 (br s)	47.0, CH	4	-	167.2, C	4	-	117.1, C	-	117.0, C
4	-	137.9, C	5	7.00 (d, 8.9)	119.5, CH	7	-	167.3, C	-	167.6, C
4-CHO	9.49 (s)	192.0, C	6	8.16 (dd, 8.9, 2.1)	138.0, CH	-OCH_3	3.92 (s)	57.0, CH_3	3.93 (s)	57.0, CH_3
5	7.11 (br d, 5.8)	151.7, CH	7	-	167.1, C	1′	4.40 (dd, 11.0, 5.2) 4.42 (dd, 11.0, 7.6)	68.1, CH_2	4.41 (dd, 11.5, 6.4) 4.61 (dd, 11.5, 2.3)	68.7, CH_2
6	2.53 (m) 2.40 (m)	24.9, CH_2	1′	-	208.1, C	2′	4.23 (m)	69.4, CH	4.02 (m)	70.5, CH
6a	2.58 (dd, 12.5, 3.7)	35.7, CH	2′	2.98 (d, 7.0)	48.2, CH_2	3′	3.59 (m)	72.3, CH	3.65 (m)	71.9, CH
7	-	41.5, C	3′	2.28 (m)	26.5, CH	4′	3.75 (m)	72.7, CH	3.94 (m)	71.5, CH
7-CH_3	1.43 (s)	19.0, CH_3	4′, 3′-CH_3	1.02 (d, 6.4)	23.0, CH_3	5′	3.65 (dd, 11.3, 5.5) 3.81 (dd, 11.3, 3.4)	65.0, CH_2	3.65 (d, 6.3)	64.6, CH_2
7-$\underline{C}H_2OH$	3.52 (d, 14.6) 3.55 (d, 14.6)	69.4, CH_2	1″	4.38 (dd, 11.0, 5.5) 4.43 (dd, 11.0, 7.3)	67.7, CH_2					
8	6.94 (d, 10.2)	161.1, CH	2″	4.23 (m)	69.4, CH					
9	6.28 (d, 10.2)	126.8, CH	3″	3.58 (dd, 8.4, 1.7)	72.3, CH					
10	-	195.3, C	4″	3.75 (m)	72.7, CH					
10a	-	58.1, C	5″	3.65 (dd, 11.3, 5.8) 3.81 (dd, 11.3, 3.7)	65.0, CH_2					
3-OH	6.63(br d, 12.4)									

flash column chromatography. FL of *H. lateritium* was collected at Nagano Prefecture Forest Research Center, and FL of *H. erinaceus* was collected at Shinshu kinoko koubou Co., Ltd.

Extraction and Isolation. FL of *H. lateritium* (257 mL) and *H. erinaceus* (820 mL) was partitioned between *n*-hexane and water and then EtOAc and water, respectively. The EtOAc-soluble part (190 mg) of FL of *H. lateritium* was fractionated by medium pressure liquid chromatography (MPLC) using gradient elution with a $CHCl_3$−MeOH mixture (silica gel, 40 g, 3.0 × 16.5 cm; 100:0, 96:4, 90:10, 80:10, 0:100) to obtain 11 fractions (HL-1 to 11). Fraction HL-5

https://doi.org/10.1021/acs.jafc.3c03633
J. Agric. Food Chem. 2023, 71, 13338−13345

(26.0 mg) was separated by reversed-phase HPLC (phenylhexyl, ϕ 20 × 250 mm, 5 mL/min, 50%MeOH) to afford compound **1** (retention time 26 min, 2.9 mg). The EtOAc-soluble part (292 mg) of FL of *H. erinaceus* was fractionated by silica gel flash column chromatography (CH_2Cl_2, 90, 80, 70, 60, 50, 40, 30, 20, and 10% CH_2Cl_2/MeOH, MeOH; 500 mL each) to obtain 16 fractions (HE-1 to 16). Fraction HE-4 (45.2 mg) was separated by reversed-phase HPLC (ODS-P, ϕ 20 × 250 mm, 5 mL/min, 40% MeOH) to afford compounds **3** (retention time 62 min, 6.6 mg) and **4** (retention time 56 min, 3.9 mg). Fraction HE-7 (21.4 mg) was separated by reversed-phase HPLC (ODS-P, ϕ 20 × 250 mm, 5 mL/min, 60% MeOH) to afford compound **2** (retention time 22 min, 1.8 mg).

Compound **1**: Pale yellow amorphous powder; $[\alpha]_D^{28}$ −36 (*c* 0.14, EtOH); IR (neat); 1681, 3364 cm^{-1}; ^1H and ^{13}C NMR, see Table 1; ESIMS *m/z* 315 $[M + Na]^+$; HRESIMS *m/z* 315.0841 $[M + Na]^+$ (calcd for $C_{15}H_{16}NaO_6$, 315.0839).

Compound **2**: White crystals; $[\alpha]_D^{25}$ −23 (*c* 1.2, MeOH); IR (neat); 1732, 3418 cm^{-1}; ^1H and ^{13}C NMR, see Table 1; ESIMS *m/z* 379 $[M + Na]^+$; HRESIMS *m/z* 379.1348 $[M + Na]^+$ (calcd for $C_{17}H_{24}NaO_8$, 379.1363).

Compound **3**: White crystals; $[\alpha]_D^{23}$ +4.9 (*c* 0.37, MeOH); IR (neat); 1711, 3383 cm^{-1}; ^1H and ^{13}C NMR, see Table 1; ESIMS *m/z* 373 $[M + Na]^+$; HRESIMS *m/z* 373.0677 $[M + Na]^+$ (calcd for $C_{14}H_{19}ClNaO_8$, 373.0661).

Compound **4**: White crystals; $[\alpha]_D^{25}$ +5.4 (*c* 0.30, MeOH); IR (neat); 1715, 3367 cm^{-1}; ^1H and ^{13}C NMR, see Table 1; ESIMS *m/z* 373 $[M + Na]^+$; HRESIMS *m/z* 373.0632 $[M + Na]^+$ (calcd for $C_{14}H_{19}ClNaO_8$, 373.0661).

^{13}C Chemical shift calculations of 1. The (3a*S*)-form of compound **1**, as well as its 3-isomer, 6a-isomer, and 7-isomer were built on Spartan'18. Those were directly subjected to NMR calculation protocol with default setting, which involved a series of conformational search, conformer narrowing, chemical shift calculations with ωB97X-D/6-31G*, empirical chemical shift corrections, and the averaging by considering the Boltzmann distribution correction based on ωB97X-V/6-311G(2df,2p)[6-311G*]//ωB97X-D/6-31G*.[1] The DP4 probability scores were calculated according to Goodman's procedure using their parameters (^{13}C: σ = 2.306 ppm, *n* = 11.38, ^1H: σ = 0.185 ppm, *n* = 14.18).[2,3] The results are summarized in Table S1.

ECD spectral calculations of 1. All calculations were performed under vacuum conditions. The set of stable conformers of compound **1** obtained in the chemical shift calculations was further optimized with B3LYP/def2-TZVP using TmoleX version 4.5.2. The following vibrational analysis with the same approximation afforded their relative free energies at 298.5 °C. These were then subjected to UV and ECD calculation with B3LYP/def2-TZVP by examining 20 excitations. The UV and ECD spectra of individual conformers were constructed based on wavelength, oscillator strength, and rotatory strength using the NORMDIST function equipped on Microsoft Excel 2016. The wavelength of the calculated UV spectrum was corrected based on the experimental UV spectrum (+6 nm) and that of the ECD spectrum was also corrected with the same value. Obtained UV and ECD spectra of individual conformers were then composited by considering the Boltzmann distribution of the conformers.

Synthesis of 3. *Methyl 4-chloro-3,5-dimethoxybenzoate (**6**).* To a stirred solution of **5** (0.51 g, 2.7 mmol) in DMF (10 mL) at room temperature (rt) were added MeI (0.70 mL, 11.2 mmol) and K_2CO_3 (1.80 g, 13.0 mmol). After being stirred for 16 h at rt, 1% hydrochloric acid (5 mL) and EtOAc (50 mL) were added to the reaction mixture. The resultant solution was washed with H_2O (20 mL × 3) and brine (20 mL × 3). The combined aqueous layer was extracted with EtOAc (30 mL × 3), and the obtained organic layers were dried over Na_2SO_4. Filtration and concentration followed by silica gel chromatography (30−55% EtOAc-hexane) afforded **6** (0.59 g, 2.6 mmol, 96% yield) as a colorless solid. The ^1H NMR data were consistent with those previously reported (Figure S19).[4]

*4-Chloro-3,5-dimethoxybenzoic acid (**7**).* To a solution of **6** (0.51 g, 2.2 mmol) in dioxane (6 mL) and H_2O (9.5 mL) were added K_2CO_3 (0.71 g, 5.1 mmol) and TBAB (11 mg, 34.1 μmol). After being refluxed overnight, the solution was acidified with concentrated hydrochloric acid and was diluted with EtOAc (100 mL). The resultant mixture was washed with H_2O (30 mL × 3) and brine (30 mL × 3). The combined aqueous layer was extracted with EtOAc (30 mL × 3), and the obtained organic layers were dried over Na_2SO_4. Filtration and concentration afforded **7** (0.46 g, 2.1 mmol, 96% yield) as a colorless solid (Figure S20). ^1H NMR (400 MHz, acetone-d_6) δ_H 7.34 (s, 2H, H-2, H-6), 3.96 (s, 6H, OCH_3); ^{13}C NMR (100 MHz, acetone-d_6) δ_C 167.2 (COOH), 157.3 (C-3, C-5), 131.0 (C-4), 116.3 (C-1), 106.8 (C-2, C-6), 57.1 (OCH_3 × 2).

*1-(2,3:4,5-Di-O-isopropyledene-D-arabinitol)-4′-chloro-3′,5′-dimethoxybenzoate (**10**).* To a stirred solution of **7** (0.10 g, 0.46 mmol) and **8** (0.12 g, 0.52 mmol) in THF (3 mL) and EtOAc (10 mL) at 0 °C were added DMAP (1.72 g, 14.1 mmol) and EDC·HCl (2.81 g, 14.7 mmol). After being refluxed for 4 h at rt, the solution was diluted with EtOAc (100 mL). The resultant mixture was washed with 1% hydrochloric acid (30 mL × 3) and brine (30 mL × 3). The combined aqueous layer was extracted with EtOAc (30 mL × 3), and the obtained organic layers were dried over Na_2SO_4. Filtration and concentration, followed by silica gel chromatography (20−70% EtOAc-hexane), afforded **10** (0.16 g, 0.37 mmol, 80% yield from **7**) as a colorless solid (Figure S21). ^1H NMR (400 MHz, $CDCl_3$) δ_H 7.29 (s, 2H, H-2′, H-6′), 4.60 (dd, *J* = 2.6, 11.9 Hz, 1H, H-1), 4.44 (dd, *J* = 5.3, 11.9 Hz, 1H, H-1), 4.28 (ddd, *J* = 2.6, 5.3, 7.9 Hz, 1H, H-2), 4.14 (dd, *J* = 6.3, 8.2 Hz, 1H, H-5), 4.08 (ddd, *J* = 4.0, 6.3, 7.9 Hz, 1H, H-4), 3.97 (dd, *J* = 4.0, 8.2 Hz, 1H, H-5), 3.92 (s, 6H, OCH_3), 3.80 (t, *J* = 7.9 Hz, 1H, H-3), 1.41 (s, 3H, CH_3), 1.39 (s, 3H, CH_3), 1.36 (s, 3H, CH_3), 1.31 (s, 3H, CH_3); ^{13}C NMR (100 MHz, $CDCl_3$) δ_C 165.7 (COOR), 156.0 (C-3′, C-5′), 128.8 (C-4′), 116.1 (C-1′), 110.1 (acetal), 109.8 (acetal), 105.7 (C-2′, C-6′), 78.5 (C-4), 77.6 (C-2), 77.1 (C-3), 67.7 (C-5), 65.1 (C-1), 56.5 (OCH_3 × 2), 27.1 (CH_3), 27.0 (CH_3), 26.7 (CH_3), 25.1 (CH_3).

*1-D-Arabinitol-4′-chloro-3′,5′-dimethoxybenzoate (synthesis of **3**).* To a stirred solution of **10** (21 mg, 48.7 μmol) in EtOH (7 mL) and H_2O (3 mL) at rt was added concentrated hydrochloric acid (0.3 mL). After being stirred for 3 h at 50 °C, the solution was cooled to rt and extracted with EtOAc (20 mL). The organic layer was washed with saturated aqueous $NaHCO_3$ solution (10 mL × 3) and brine (10 mL × 3). The combined aqueous layer was extracted with EtOAc (10 mL × 3), and the obtained organic layers were dried over Na_2SO_4. Filtration and concentration followed by silica gel chromatography (2−16% MeOH−$CHCl_3$) afforded **3** (13 mg, 37.1 μmol, 76% yield) as a colorless solid. The ^1H NMR and ^{13}C NMR data were fully consistent with those of the natural product (Figures S22 and S23).

Syntheses of 11 and 12. To a stirred solution of 4-bromo-3,5-dimethoxybenzoic acid (100 mg) in anhydrous pyridine (600 μL) was added *N*,*N*′-dicyclohexylcarbodiimide, DCC (15 mg). After the solution was stirred for 30 min, D-(+)-arabitol (100 mg) was added to the solution, and the reaction mixture was stirred for 96 h at room temperature. After adding water to the mixture, it was extracted with EtOAc for three times. The combined EtOAc solution was dried over anhydrous Na_2SO_4, filtered, and dried under reduced pressure. The residue was fractionated by reversed-phase HPLC (PBr, 35% MeOH) to afford **11** (6.0 mg) and **12** (5.7 mg) (Figures S24−27).

Compound **11**: $[\alpha]_D^{24}$ +4.2 (*c* 0.10, MeOH)

Compound **12**: $[\alpha]_D^{26}$ +4.1 (*c* 0.40, MeOH)

X-ray Crystallography Analyses of 2 and 3. Compound **2** was crystallized in MeOH. Single crystal was mounted on MiTeGen loop with Paraton-N (Hampton Research) and was flash frozen to 173 K in a liquid nitrogen-cooled stream of nitrogen. Data collection was carried out on a Rigaku XtaLAB Synergy-S diffractometer using a multilayer mirror monochromated Cu microfocus sealed X-ray source (50 W) and a Hypix-6000 Hybrid Photon Counting (HPC) detector. Data collection and reduction were made using the CrysAlis PRO softwater package. The structure was solved by a direct method, ShelXT, and refined using the SHELX97 tool. All of the nonhydrogen atoms were refined anisotropically. The hydrogen atoms were placed in calculated positions and allowed to ride on the carrier atoms. The absolute structure was estimated based on the Flack parameter.

https://doi.org/10.1021/acs.jafc.3c03633
J. Agric. Food Chem. 2023, 71, 13338−13345

Crystallographic data have been deposited at the Cambridge Crystallographic Data Centre and assigned the deposition number CCDC 2080028. The data can be obtained free of charge via www.ccdc.cam.ac.uk/produts/csd/request. The size of the crystal used for measurements was 0.38 × 0.01 × 0.01 mm. Crystal data and the detailed structure determination of **2** are summarized in Table S2.

Compound **3** was crystallized in 2-propanol. Single crystals were measured by the same method of **2**. Crystallographic data have been deposited at the Cambridge Crystallographic Data Centre and allocated the deposition number CCDC 2114934. The size of the crystal used for measurements was 0.08 × 0.05 × 0.02 mm. Crystal data and the detailed structure determination of **3** are summarized in Table S2.

Biological activity assay. *Fruiting-body formation assay.* The mycelia of *F. velutipes* were placed on a potato dextrose agar (PDA) plate. Meanwhile, each test compound solution was poured onto autoclaved paper disks (Advantec, ϕ 8 mm) and then air-dried. Each air-dried paper disk containing 1 μmol/paper disk of the compounds was placed directly onto the incubated plate (n = 3). Plates were further incubated at 25 °C for 1 week. After the incubation, the activity was evaluated by observation of the fruiting-body formation.

Hypoxia-Inducible Factor Assay. Cell culture. The murine cell lines for fibroblast 3T3 and cone photoreceptor 661W were cultured in DMEM (cat. #08456−36, Nacalai Tesque, Japan) media supplemented with 10% FBS and 1% streptomycin-penicillin at 37 °C under an atmosphere containing 5% CO_2. The human cell line for retinal epithelial ARPE-19 was cultured in DMEM/F-12 (catalog no. C11330500BT, Gibco, USA) media with the supplements the same as above. These cells were continuously maintained until experiments.

Luciferase assay. A luciferase assay was performed as previously described.[5] Briefly, 3T3, 661W and ARPE-19 cell lines were transfected with a HIF-luciferase reporter gene construct (Cignal Lenti HIF Reporter, Qiagen, Netherlands). The HIF-luciferase construct encodes a firefly luciferase gene under the control of HRE which binds HIF. The cell lines were also cotransfected with a cytomegalovirus-renilla luciferase construct as an internal control and seeded at 1.0 × 10^4 cells/well/70 μL (3T3 and ARPE-19) or 0.8 × 10^4 cells/well/70 μL (661W) in a white sterile HTS Transwell-96 receiver plate (Corning, NY, USA). At 24 h of cell stabilization, the cells were treated with $CoCl_2$ (200 mM, cobalt(II) chloride hexahydrate, Wako, Saitama, Japan) to activate HIF. To evaluate the inhibitory effects of test compounds (1 mg/mL) against HIF activation, the cells were cotreated with each compound and $CoCl_2$. After incubation for 24 h at 37 °C in a 5% CO_2 incubator, luminescence was measured using a Dual-Luciferase Reporter Assay System (Promega, Madison, WI, USA). One mM of Topotecan (Cayman Chemical, Ann Arbor, MI, USA) and 1 mM of doxorubicin (Tokyo Chemical Industry Co., Ltd., Tokyo, Japan) were used for expected HIF inhibitory positive controls.

Statistical analysis. Analyses of data from all experiments were performed with GraphPad Prism 5 (GraphPad Software, San Diego, CA, USA). Statistical significance was calculated using a two-tailed Student's t-test or one-way ANOVA followed by a Bonferroni post hoc test. p-Values less than 0.05 were considered statistically significant.

Axl assay. The human A549 alveolar epithelial cell line was purchased from the American Type Culture Collection (Rockville, MD, USA) and cultured in Dulbecco's modified Eagle's medium (DMEM), supplemented with 10% heat-inactivated fetal bovine serum, 2 mM L-glutamine and 100 U/mL penicillin plus 100 U/mL streptomycin. All cells were cultured at 37 °C in 75 cm^2 flasks under an atmosphere composed of 5% CO_2 and 95% air. Confluent cells were passaged after 5−7 days. A549 cells in 0.1% Bovine serum albumin (BSA) and DMEM were seeded in 24-well plates. Each of the compounds **2**−**4** (20 μg/mL) was added to the wells, and the plates were incubated for 24 h. Total RNA was extracted using Sepasol -RNA I Super G (Nacalai) following the instructions of the manufacturer. One μg of total RNA was denatured at 65 °C for 10 min and then reverse-transcribed using ReverTra Ace Reverse Transcriptase (TOYOBO) and oligo (dT) primer in a volume of 20 μL according to the manufacturer's protocol. Each gene contains forward and reverse sequeance (5′ > 3′) as GGAGCGA-GATCCCTCCAAAAT and GGCTGTTGTCATACTTCTCATGG for the GADPH gene and TGCCATTGAGAGTCTAGCTGAC and TTAGCTCCCAGCACCGCGAC for the Axl gene. The cDNA was amplified by PCR, and the conditions were as follows: 94 °C, 1 min; 60 °C, 1 min; and 72 °C, 1 min for 28−35 cycles. PCR products were electrophoresed on a 1.5% agarose gel and then stained with ethidium bromide solution. Semiquantitative RT-PCR results were quantified by using ImageJ software. The statistical difference was calculated by analysis of variance with post hoc analysis using Fisher's protected least significant difference test.

RESULTS AND DISCUSSION

FL of *H. lateritium* (257 mL) and *H. erinaceus* (820 mL) were collected from about 2,000 and 6,000 pots using a suction pump, respectively (Figure 1), and partitioned between *n*-hexane and water and then EtOAc and water. Each EtOAc-soluble part was fractionated by repeated chromatography. As a result, compound **1** and compounds **2**−**4** were isolated from FL of *H. lateritium* and *H. erinaceus*, respectively (Figure 2).

Compound **1** was purified as a pale yellow, amorphous powder. The molecular formula was determined as $C_{15}H_{16}O_6$ by HRESIMS (m/z 315.0841 $[M + Na]^+$; calcd for $C_{15}H_{16}NaO_6$, 315.0839), indicating the presence of eight degrees of unsaturation in the molecule. The structure of **1** was elucidated by interpretation of NMR spectra including DEPT, HMQC, COSY, and HMBC (Figures S2−S5). The DEPT experiment indicated the presence of one methyl, two methylenes, seven methines, and five tetrasubstituted carbons. The complete assignment of all of the protons and carbons was accomplished as shown in Table 1. ^{13}C NMR chemical shift of C-1 (δ_C 170.9), the HMBC correlations (H-3/C-1, C-10a; H-3a/C-1, C-3, C-10a), and the COSY correlation (H-3/3-OH)

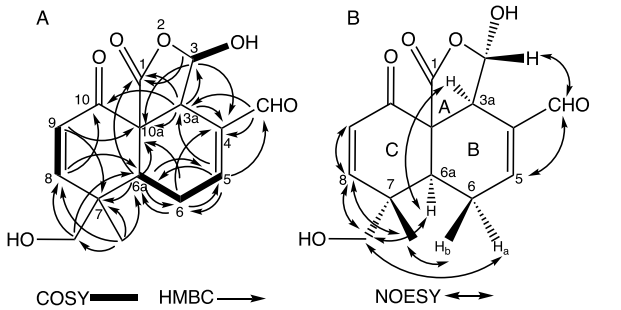

Figure 3. COSY, HMBC (A), and NOSEY (B) correlations of **1**.

suggested partial structure A with an ester bond (Figure 3A). ^1H and ^{13}C NMR chemical shifts [δ_H 9.49 (s, 1H), δ_C 192.0], the HMBC correlations (H-3a/C-4, C-10a; −CHO/C-4, C-3a; H-5/C-3a, C-6, C-6a, −CHO; H-6/C-4, C-5, C-6a, C-10a; H-6a/C-5, C-6, C-10a), and the COSY correlations (H-5/H-6, H-6/H-6a) suggested partial structure B with a formyl group (Figure 3A). The HMBC correlations (H-9/C-7, C-10a; H-8/C-10, C-6a; H-6a/C-7; 7-CH_3/C-6a, C-7, C-8, 7-$\underline{C}H_2OH$; 7-$C\underline{H}_2OH$/C-8, C-6a) and the COSY correlation (H-8/H-9) suggested partial structure C containing a carbonyl group (δ_C 195.3), a double bond between C-8 and C-9 [δ_H 6.94 (d, J = 10.2 Hz, 1H), δ_C 161.1; δ_H 6.28 (d, J = 10.2 Hz, 1H), δ_C 126.8], and a hydroxymethyl at C-7 [δ_H 3.52 (d, J = 14.6 Hz, 1H); δ_H 3.55 (d, J = 14.6 Hz, 1H), δ_C 69.4] (Figure 3A). The linkages of the three parts were elucidated by the HMBC

https://doi.org/10.1021/acs.jafc.3c03633
J. Agric. Food Chem. 2023, 71, 13338−13345

correlations (H-3/C-4; H-3a/C-10; H-6a/C-1) (Figure 3A). The relative stereochemistry except for C-3 of **1** was determined by the NOESY correlations (H-3a/H-6a; H-6*a*/7-CH_2OH; H_a-6/7-CH_2OH; H_b-6/7-CH_3) as depicted in Figure 3B. The whole absolute configurations of **1** were determined by DFT-based chemical shift calculations. DFT-based ^{13}C chemical shift calculations for **1** afforded a small enough root-mean-square of deviation from the experimental data (1.6 ppm) and exclusively high DP4 scores (^{13}C: 94.1%, ^{1}H, 100%, $^{13}C+^{1}H$: 100%) among eight diastereomers regarding C-3, C-6a, and C-7, when Goodman's parameters were employed (Tables S1).[2,3] This compound afforded a negative Cotton effect ($\Delta\varepsilon$ −5.3) at 239 nm and a positive Cotton effect ($\Delta\varepsilon$ + 3.6) at 200 nm in the ECD spectrum (Figure 4). These were in accordance with the UV absorption

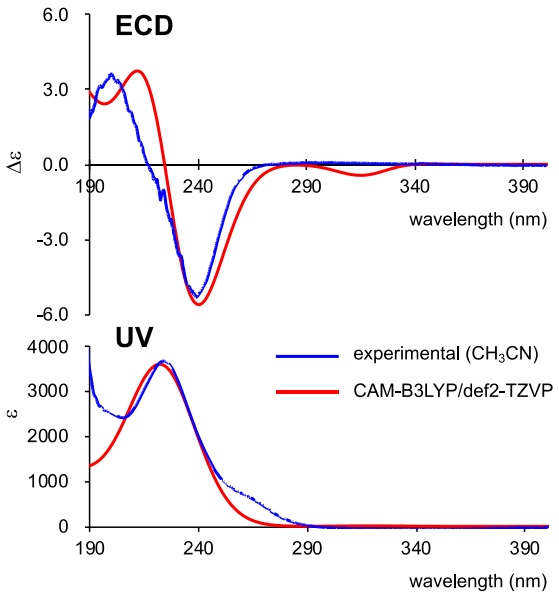

Figure 4. Comparison of the calculated ECD spectra at the B3LYP/def2-TZVP level with the experimental spectra of **1** in CH_3CN.

at 230 nm due to *α*,*β*-unsaturated carbonyl groups (C-5/C-4/CHO, and C-8/C-9/C-10). Since the dihedral angle between C-4/C-5 and C-8/C-9 double bonds are −6.3° in the (3a*S*)-enantiomer, we assumed these two chromophores caused the negatively splitting ECD coupling. DFT calculations of (3a*S*)-**1** nicely reproduced the ECD spectrum, confirming the (3a*S*)-enantiomer of **1**. Therefore, the absolute configuration of compound **1** is (3*S*,3a*S*,6a*S*,7*R*,10a*R*).

Compound **2** was purified as white crystals. The molecular formula was determined as $C_{17}H_{24}O_8$ by HRESIMS (*m*/*z* 379.1348 $[M + Na]^+$; calcd for $C_{17}H_{24}NaO_8$, 379.1363), indicating the presence of six degrees of unsaturation in the molecule. The structure of **2** was elucidated by interpretation of NMR spectra including DEPT, HMQC, COSY, and HMBC (Figures S7−S10). The DEPT experiment indicated the presence of two methyls, three methylenes, seven methines, and five tetrasubstituted carbons. The complete assignment of all the protons and carbons was accomplished as shown in Table 1. The 1,2,4-substituted benzoate skeleton was constructed based on the characteristic ^{1}H and ^{13}C NMR chemical shifts and coupling constants at [δ_C 120.8; δ_H 8.59 (d, *J* = 2.1 Hz, 1H), δ_C 134.1; δ_C 122.3; δ_C 167.2; δ_H 7.00 (d, *J* = 8.9 Hz, 1H), δ_C 119.5; δ_H 8.16 (dd, *J* = 8.9, 2.1 Hz, 1H), δ_C 138.0; δ_C 167.1] and the HMBC correlations (H-2/C-4, C-6, C-7; H-5/C-3, C-4; H-6/C-2, C-4, C-7) (Figure 5). 3-

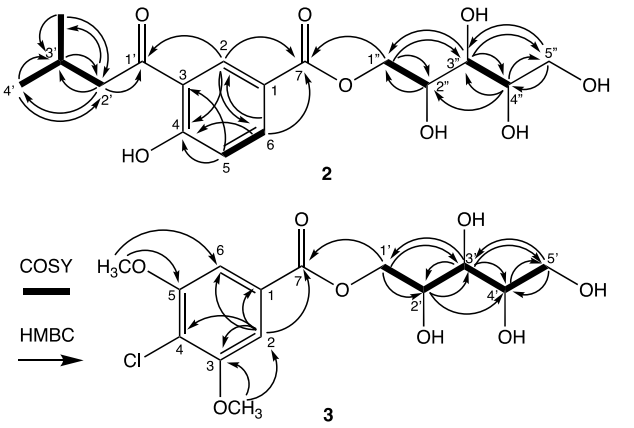

Figure 5. COSY and HMBC correlations of **2** and **3**.

Methylbutanone moiety attached to C-3 was elucidated by the HMBC correlations (H-2/C-1′; H-2′/C-1′, C-3′, C-4′, 3′-CH_3; H-3′/C-2′; H-3′-CH_3/C-2′, C-3′; H-4′/C-2′, C-3′) (Figure 5). Additionally, the HMBC correlations (H-1″/C-7, C-2″, C-3″; H-2″/C-1″; H-3″/C-1″, C-4″, C-5″; H-4″/C-2″, C-3″, C-5″; H-5″/C-3″, C-4″) suggested the presence of a sugar alcohol at C-7 (Figure 5). Confirmation of the structure and determination of the absolute configuration of **2** were performed by X-ray crystallography analysis (Figure 6A). As a result, the sugar alcohol was D-arabinitol and **2** was determined as (2*R*,3*R*,4*R*)-2,3,4,5-tetrahydroxypentyl 4-hydroxy-3-(3-methylbutanoyl)benzoate (Figure 2).

Compound **3** was obtained as white crystals. The molecular formula was determined as $C_{14}H_{19}ClO_8$ by HRESIMS (*m*/*z* 373.0677 $[M + Na]^+$; calcd for $C_{14}H_{19}ClNaO_8$, 373.0661), indicating the presence of five degrees of unsaturation in the molecule. The structure of **3** was elucidated by interpretation of NMR spectra including DEPT, HMQC, COSY, and HMBC (Figures S11−S14). The DEPT experiment indicated the presence of two methyls, two methylenes, five methines, and five tetrasubstituted carbons. The complete assignment of all the protons and carbons was accomplished as shown in Table 1. The four substituted symmetric benzoate moiety was elucidated by its NMR chemical shifts [δ_C 130.6; δ_H 7.38 (s, 2H), δ_C 106.7; δ_C 157.5; δ_C 117.1; δ_C 167.3] and the HMBC correlations (H-2/C-1, C-3, C-4, C-6, C-7) (Figure 5). The positions of the methoxy groups were determined by the HMBC correlation from the protons to C-3 and C-5 (H-3OCH_3/C-2, C-3; H-5OCH_3/C-5, C-6). The sugar alcohol moiety was determined by the COSY correlations (H-1′/H-2′; H-2′/H-3′; H-3′/H-4′; H-4′/H-5′) and the HMBC correlations (H-1′/C-2′, C-3′, C-7; H-2′/C-3′, C-4′; H-3′/C-1′, C-2′, C-4′, C-5′; H-4′/C-5′; H-5′/C-3′, C-4′) (Figure 5). In addition, ^{1}H and ^{13}C NMR chemical shifts of the pentanol part of **3** were almost the same as those of the corresponding part in **2**, indicating that the pentanol was arabinitol. Furthermore, the determination of the absolute configuration of **3** was performed by chemical synthesis. Commercially available **5** was methylated by using MeI under basic conditions (Scheme 1). As a result, ester **6** was yielded in 96%. Carboxylic acid **7** was synthesized in an excellent yield from **6** via saponification in the presence of tetrabutylammonium bromide (TBAB) as a phase-transfer catalyst. D-

https://doi.org/10.1021/acs.jafc.3c03633
J. Agric. Food Chem. 2023, 71, 13338−13345

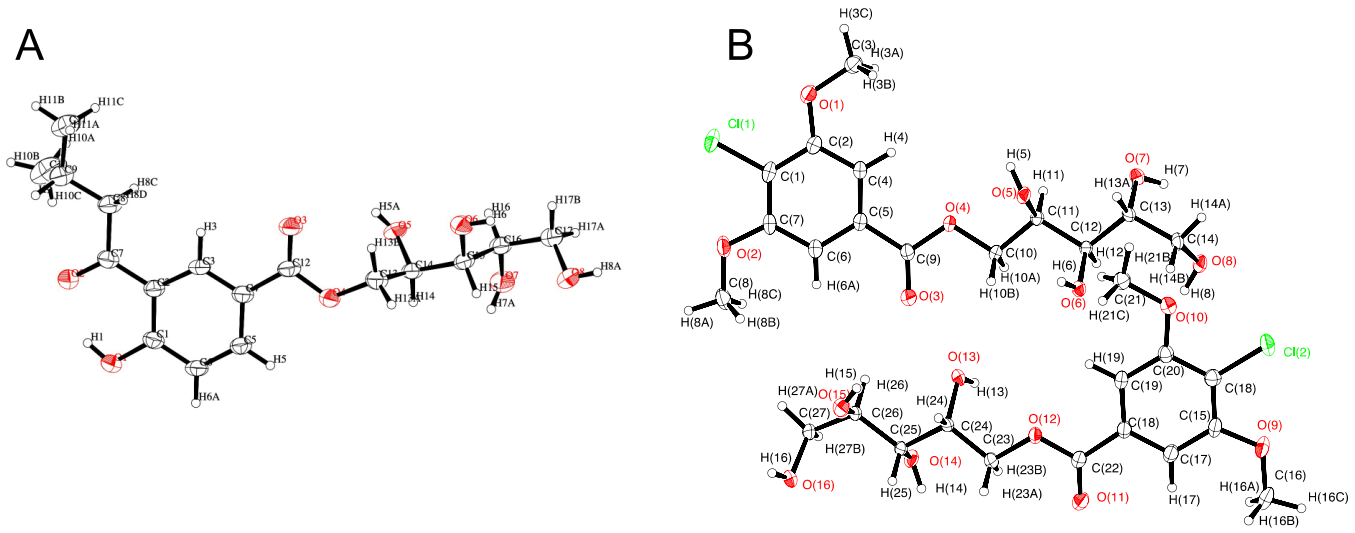

Figure 6. ORTEP drawings of **2** (A) and **3** (B) with ellipsoids at the 30% probability level. Hydrogen atoms are shown as small spheres of arbitrary radii.

Scheme 1. Synthesis of 3

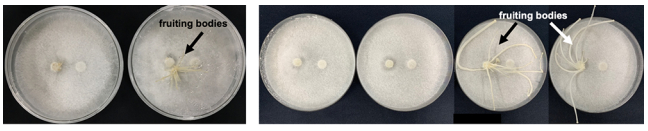

(−)-Mannitol (**8**) was converted to alcohol **9** in 26% yield over four steps.[6] The esterification of **7** with **9** by using 1-(3-(dimethylamino)propyl)-3-ethylcarbodiimide hydrochloride (EDC·HCl) afforded ester **10** in 80% yield. Finally, **10** was transformed into **3** in 76% yield by acid hydrolysis. Consequently, **3** was synthesized for the first time from **5** in a 56% yield over four steps. The ^{1}H NMR and ^{13}C NMR data of synthesized **3** were fully consistent with those of the natural product (Figures S22 and S23). Furthermore, X-ray crystallography analysis of natural **3** confirmed the absolute configuration (Figure 6B). All the above data indicated that the sugar alcohol was also D-arabinitol, and **3** was determined as (2*R*,3*R*,4*R*)-2,3,4,5-tetrahydroxypentyl 4-chloro-3,5-dimethoxybenzoate (Figure 2).

Compound **4** was obtained as white crystals. The molecular formula was determined to be the same as that for **3** ($C_{14}H_{19}ClO_8$) by HRESIMS (*m*/*z* 373.0632 [M + Na]$^+$; calcd for $C_{14}H_{19}ClNaO_8$, 373.0661). The ^{1}H and ^{13}C NMR spectral analyses uncovered that **4** is a diastereomer of **3**. We assumed that **4** possesses the same unit (D-arabinitol) by taking the occurrence of the same source into account. Therefore, we attempted to synthesize Br-analogues of **3** and **4** by condensation between commercially available 4-bromo-3,5-dimethoxybenzoic acid and D-(+)-arabitol because we thought that the arabitol moieties of Br-analogues would give NMR chemical shifts very similar to those of **3** and **4**. The reaction afforded a set of monoesters **11** and **12**, and as expected, **11** and **12** gave almost the same ^{1}H and ^{13}C NMR spectra as those of **3** and **4** except for the chemical shifts of the phenyl groups, respectively (Figures S24−S27). Comparisons of the specific rotations of **3** {$[\alpha]_D^{23}$ +4.9 (*c* 0.37, MeOH)} and **11** {$[\alpha]_D^{24}$ +4.2 (*c* 0.10, MeOH)} with those of **4** {$[\alpha]_D^{24}$ +5.4 (*c* 0.30, MeOH)} and **12** {$[\alpha]_D^{24}$ +4.1 (*c* 0.40, MeOH)} allowed us to conclude that the absolute configuration of **4** is (2′*R*,3′*S*,4′*R*) (Figure 2).

Fruiting body development in basidiomycetes is induced not only by the environmental and physical stimuli but also by various chemicals.[7] Basidifferquinones isolated from *Streptomyces* sp. induced the fruiting-bodies of basidiomycetes *Favolus arcularius* and *Polyporus arcularius*.[8,9] Adenosine 3′,5′-cyclic monophosphate (cyclic AMP) induced the fruiting bodies of *Coprinus macrorhizus*.[10] As mentioned above, we hypothesized that the liquid plays an important role(s) in fruiting-body formation; therefore, the effect of compounds **1**−**4** on fruiting-body induction against *Flammulina velutipes* was evaluated. Among them, compounds **1**, **3**, and **4** induced fruiting-body formation at 1 μmol/paper disk after 2 months (Figure 7).

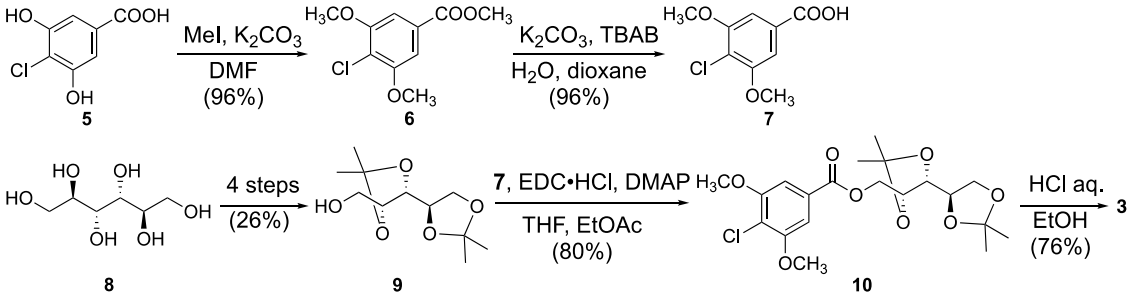

Figure 7. Effect of compounds **1** to **4** on the fruiting-body formation at 1 μmol/paper disk for 2 months.

https://doi.org/10.1021/acs.jafc.3c03633
J. Agric. Food Chem. 2023, 71, 13338−13345

We also examined the effect of the compounds on the hypoxia-inducible factor (HIF) by a luciferase assay. HIF is a transcriptional factor that has a pivotal role in the cellular adaptive response to a hypoxic condition. Stabilization and activation of HIF induces cell survival under hypoxia including neovascularization, cell respiration, apoptosis, glucose metabolism, and embryogenesis.[11] We have focused on the role of HIF in retinal homeostasis and revealed that HIF inhibition may be effective against retinal neovascular and neurodegeneration.[12] Compounds **2** and **4** were subjected to the assay using the 3T3, 661W, and ARPE-19 cell lines, and **4** showed an HIF inhibitory effect (Figure S28).

Also, the effect of the compounds on the expression of a receptor tyrosine kinase (Axl) was evaluated. The Axl receptor tyrosine kinase is involved in tumor growth and metastasis, and its overexpression is an indicator of poor prognosis in several malignant tumors, including lung cancer.[13] Axl also plays an important role in the epithelial-mesenchymal transition (EMT), an important step for the initiation of metastasis and the development of resistance to drug and chemotherapy.[14] Axl has been clinically reported as one of the promising targets in cancer treatment.[15] Therefore, if the expression of Axl was downregulated by a small compound, the compound might become a promising candidate as an anticancer reagent. The inhibitory activity of compounds **2**−**4** on Axl mRNA expression was evaluated in the human A549 alveolar epithelial cell line by PCR. All the compounds significantly inhibited the expression of Axl (Figure S29).

We named the liquid that appears on mycelia's surface immediately prior to the formation of fruiting bodies of mushroom-forming fungi as the "fruiting liquid (FL)". Four novel compounds (**1**−**4**) were discovered from FL of *H. lateritium* and *H. erinaceus*. Triterpenes and steroids have been isolated from the fruiting bodies of *H. lateritium;* however, any sesquiterpenes such as **1** have never been isolated from this fungus.[16,17] Among the metabolites of *H. erinaceus*, chlorinated orcinol derivatives were produced from the culture broth and scrap cultivation beds of this fungus.[18−20] However, sugar alcohol analogs like **2**−**4** were isolated from *H. erinaceus* for the first time. Compounds **1**, **3**, and **4** induced fruiting bodies of *F. velutipes*. In the mushroom industry, there is a great call for artificial control of the timing of the formation of fruiting bodies from mycelia. Fruiting-body inducers like **1**, **3**, and **4** might be able to contribute to the industry. We are now examining the effects of the compounds on other edible mushroom-forming fungi and searching for other inducers from the two FL and other kinds of FL. In addition, compound **4** inhibited the activity of HIF and compounds **2**−**4** suppressed Axl expression. Guttation is a well-known phenomenon in plants and fungi that involves the active exudation of water and dissolved substances without tissue injury.[21,22] There are some reports that guttation in filamentous fungi occurs at different conditions, and its ecological role is elusive.[23] The components of guttation in filamentous fungi have been identified to be carboxylic acids, carbohydrates, fatty acids, and amino acids by GC-MS or LC-MS/MS.[24,25] However, to the best of our knowledge, this study is the first to focus on FL scientifically and discover new compounds from guttation including FL.

■ ASSOCIATED CONTENT

Supporting Information

The Supporting Information is available free of charge at https://pubs.acs.org/doi/10.1021/acs.jafc.3c03633.

FL of mushroom-forming fungi (Figure S1), 1D and 2D NMR spectra of **1**−**4**, **6**, **7**, and **10**−**12** (Figures S2−S27), ECD data of **1** (Table S1), crystallographic data of **2** and **3** (Table S2), and bioassay (Figures S28 and S29) (PDF)

■ AUTHOR INFORMATION

Corresponding Author

Hirokazu Kawagishi − *Faculty of Agriculture and Research Institute for Mushroom Science, Shizuoka University, Shizuoka 422-8529, Japan;* orcid.org/0000-0001-5782-4981; Phone: +81-54-238-4885; Email: kawagishi.hirokazu@shizuoka.ac.jp

Authors

Jing Wu − *Faculty of Agriculture and Research Institute for Mushroom Science, Shizuoka University, Shizuoka 422-8529, Japan*

Kazuki Uchida − *Graduate School of Integrated Science and Technology, Shizuoka University, Shizuoka 422-8529, Japan*

Aoto Yoshikawa − *Graduate School of Integrated Science and Technology, Shizuoka University, Shizuoka 422-8529, Japan*

Masaru Hashimoto − *Faculty of Agriculture and Life Science, Hirosaki University, Aomori 036-8561, Japan;* orcid.org/0000-0002-4508-2105

Mitsuru Kondo − *Research Institute of Green Science and Technology, Shizuoka University, Shizuoka 422-8529, Japan;* orcid.org/0000-0002-3946-6882

Kenichi Nihei − *Department of Applied Biological Chemistry, School of Agriculture, Utsunomiya University, Tochigi 321-0943, Japan*

Mizuki Ishii − *Department of Applied Biological Chemistry, School of Agriculture, Utsunomiya University, Tochigi 321-0943, Japan*

Jae-Hoon Choi − *Faculty of Agriculture, Research Institute for Mushroom Science, Graduate School of Integrated Science and Technology, and Research Institute of Green Science and Technology, Shizuoka University, Shizuoka 422-8529, Japan*

Yukihiro Miwa − *Laboratory of Photobiology and Department of Ophthalmology, Keio University School of Medicine, Tokyo 160-8582, Japan;* orcid.org/0000-0002-5377-6772

Chiho Shoda − *Laboratory of Photobiology and Department of Ophthalmology, Keio University School of Medicine, Tokyo 160-8582, Japan*

Deokho Lee − *Laboratory of Photobiology and Department of Ophthalmology, Keio University School of Medicine, Tokyo 160-8582, Japan*

Ayaka Nakai − *Laboratory of Photobiology and Department of Ophthalmology, Keio University School of Medicine, Tokyo 160-8582, Japan*

Toshihide Kurihara − *Laboratory of Photobiology and Department of Ophthalmology, Keio University School of Medicine, Tokyo 160-8582, Japan*

Corina N. D'Alessandro-Gabazza − *Department of Immunology, Mie University Graduate School of Medicine, Tsu, Mie 524-8507, Japan*

Masaaki Toda − *Department of Immunology, Mie University Graduate School of Medicine, Tsu, Mie 524-8507, Japan*

Taro Yasuma − *Department of Immunology, Mie University Graduate School of Medicine, Tsu, Mie 524-8507, Japan*
Esteban C. Gabazza − *Department of Immunology, Mie University Graduate School of Medicine, Tsu, Mie 524-8507, Japan*
Hirofumi Hirai − *Faculty of Agriculture, Research Institute for Mushroom Science, Graduate School of Integrated Science and Technology, and Research Institute of Green Science and Technology, Shizuoka University, Shizuoka 422-8529, Japan*

Complete contact information is available at: https://pubs.acs.org/10.1021/acs.jafc.3c03633

Funding

This work was partially supported by JST, ACT-X Grant Number JPMJAX2115, Japan, and by Specific Research Grant from Takeda Science Foundation.

Notes

The authors declare no competing financial interest.

■ ACKNOWLEDGMENTS

We thank Prof. M. Arai (Keio University) for valuable discussion, M. Kubo (Shinshu kinoko koubou Co., Ltd.) and K. Masuno (Nagano Prefecture Forest Research Center) for providing fruiting liquid.

■ REFERENCES

(1) *Tutorial and User's Guide, Spartan'18 for Windows, Macintosh and Linux*; Wavefunction Inc. 2016.
(2) Hehre, W.; Klunzinger, P.; Deppmeier, B.; Driessen, A.; Uchida, N.; Hashimoto, M.; Fukushi, E.; Takata, Y. Efficient protocol for accurately calculating ^{13}C chemical shifts of conformationally flexible natural products: scope, assessment, and limitations. *J. Nat. Prod.* **2019**, *82*, 2299−2306.
(3) Smith, S. G.; Goodman, J. M. Assigning stereochemistry to single diastereoisomers by GIAO NMR calculation: the DP4 probability. *J. Am. Chem. Soc.* **2010**, *132*, 12946−12959.
(4) Kompis, I.; Wick, A. Synthesis of a 4 halo substituted analogue of trimethoprim. *Helv. Chim. Acta* **1977**, *60*, 3025−3034.
(5) Kunimi, H.; Miwa, Y.; Inoue, H.; Tsubota, K.; Kurihara, T. A novel HIF inhibitor halofuginone prevents neurodegeneration in a murine model of retinal ischemia-reperfusion. *Int. J. Mol. Sci.* **2019**, *20*, 3171−3189.
(6) Richter, J. M.; Whitefield, B. W.; Maimone, T. J.; Lin, D. W.; Castroviejo, M. P.; Baran, P. S. Scope and mechanism of direct indole and pyrrole couplings adjacent to carbonyl compounds: Total synthesis of acremoauxin A and oxazinin 3. *J. Am. Chem. Soc.* **2007**, *129*, 12857−12869.
(7) Uno, I.; Ishikawa, T. Purification and identification of the fruiting-inducing substances in *Coprinus macrorhizus*. *J. Bacteriol.* **1973**, *113*, 1240−1248.
(8) Azuma, M.; Yoshida, M.; Horinouchi, S.; Beppu, T. Basidifferquinone analogues, basidifferquinone B and C, which induce fruiting-body formation of a basidiomycete. *Favolus arcularius. Biosci. Biotechnol. Biochem.* **1993**, *57*, 344−345.
(9) Hashimoto, T.; Tashiro, T.; Kitahara, T.; Mori, K.; Sasaki, M.; Takikawa, H. First synthesis of (±)-basidifferquinone C, an inducer for fruiting-body formation in *Polyporus arcularius*. *Biosci. Biotechnol. Biochem.* **2009**, *73*, 2299−2302.
(10) Uno, I.; Ishikawa, T. Metabolism of adenosine 3′,5′-cyclic monophosphate and induction of fruiting bodies in *Coprinus macrorhizus*. *J. Bacteriol.* **1973**, *113*, 1249−1255.
(11) Kaelin, W. G.; Ratcliffe, P. J. Oxygen sensing by metazoans: The central role of the HIF hydroxylase pathway. *Mol. Cell* **2008**, *30*, 393−402.
(12) Lee, D.; Miwa, Y.; Wu, J.; Shoda, C.; Jeong, H.; Kawagishi, H.; Tsubota, K.; Kurihara, T. A fairy chemical suppresses retinal angiogenesis as a HIF inhibitor. *Biomolecules* **2020**, *10*, 1405−1418.
(13) Tsukita, Y.; Fujino, N.; Miyauchi, E.; Saito, R.; Fujishima, F.; Itakura, K.; Kyogoku, Y.; Okutomo, K.; Yamada, M.; Okazaki, T.; Sugiura, H.; Inoue, A.; Okada, Y.; Ichinose, M. and Ichinose, Axl kinase drives immune checkpoint and chemokine signalling pathways in lung adenocarcinomas. *Mol. Cancer* **2019**, *18*, 24−29.
(14) Zhu, C.; Wei, Y.; Wei, X. AXL receptor tyrosine kinase as a promising anti-cancer approach: functions, molecular mechanisms and clinical applications. *Mol. Cancer* **2019**, *18*, 153−174.
(15) Rankin, E. B.; Giaccia, A. J. The receptor tyrosine kinase Axl in cancer progression. *Cancers* **2016**, *8*, 103−118.
(16) Chuluunbaatar, B.; Béni, Z.; Dékány, M.; Kovács, B.; Sárközy, A.; Datki, Z.; Mácsai, L.; Kálmán, J.; Hohmann, J.; Ványolós, A. Triterpenes from the mushroom *Hypholoma lateritium*: isolation, structure determination and investigation in bdelloid rotifer assays. *Molecules* **2019**, *24*, 301−310.
(17) Ványolós, A.; Muszyńska, B.; Chuluunbaatar, B.; Gdula-Argasińska, J.; Kała, K.; Hohmann, J. Extracts and steroids from the edible mushroom *Hypholoma lateritium* exhibit anti-inflammatory properties by inhibition of COX-2 and activation of Nrf2. *Chem. Biodivers.* **2020**, *17*, No. e2000391.
(18) Okamoto, K.; Sakai, T.; Shimada, A.; Shirai, R.; Sakamoto, H.; Yoshida, S.; Ojima, F.; Ishiguro, Y.; Kawagishi, H. Antimicrobial chlorinated orcinol derivatives from mycelia of *Hericium erinaceum*. *Phytochemistry* **1993**, *34*, 1445−1446.
(19) Wu, J.; Tokunaga, T.; Kondo, M.; Ishigami, K.; Tokuyama, S.; Suzuki, T.; Choi, J.-H.; Hirai, H.; Kawagishi, H. Erinaceolactones A to C, from the culture broth of *Hericium erinaceus*. *J. Nat. Prod.* **2015**, *78*, 155−158.
(20) Ueda, K.; Kodani, S.; Kubo, M.; Masuno, K.; Sekiya, A.; Nagai, K.; Kawagishi, H. Endoplasmic reticulum (ER) stress-suppressive compounds from scrap cultivation beds of the mushroom *Hericium erinaceum*. *Biosci. Biotechnol. Biochem.* **2009**, *73*, 1908−1910.
(21) Ivanoff, S. S. Guttation injuries of plants. *Bot. Rev.* **1963**, *29*, 202−229.
(22) Colotelo, N. Fungal exudates. *Can. J. Microbiol.* **1978**, *24*, 1173−1181.
(23) Krain, A.; Siupka, P. Fungal guttation, a source of bioactive compounds, and its ecological role−A review. *Biomolecules* **2021**, *11*, 1270−1286.
(24) Aliferis, K. A.; Jabaji, S. Metabolite composition and bioactivity of *Rhizoctonia solani* sclerotial exudates. *J. Agric. Food Chem.* **2010**, *58*, 7604−7615.
(25) Salo, M. J.; Marik, T.; Mikkola, R.; Andersson, M. A.; Kredics, L.; Salonen, H.; Kurnitski, J. *Penicillium expansum* strain isolated from indoor building material was able to grow on gypsum board and emitted guttation droplets containing chaetoglobosins and communesins A, B and D. *Appl. Microbiol.* **2019**, *127*, 1135−1147.